Yan-Feng Li, Zhiqiang Lv, Wei Cai, Shun-Peng Zhu and Hong-Zhong Huang*

Fatigue Life Analysis of Turbine Disks Based on Load Spectra of Aero-engines

Abstract: Load spectra of aero-engines reflect the process of operating aircrafts as well as the changes of parameters of aircrafts. According to flight hours and speed cycle numbers of the aero-engines, the relationship between load spectra and the fatigue life of main components of the aero-engines is obtained. Based on distribution function and a generalized stress–strength interference model, the cumulative fatigue damage of aero-engines is then calculated. After applying the analysis of load spectra and the cumulative fatigue damage theory, the fatigue life of the first-stage turbine disks of the aero-engines is evaluated by using the *S–N* curve and Miner's rule in this paper.

Keywords: fatigue life, stress–strength interference model, load spectra, aero-engines, turbine disks

PACS®(2010). 02.50.-r, 02.50.Fz, 46.50.+a, 62.20.me, 88.40.fm

DOI 10.1515/tjj-2015-0004
Received January 16, 2015; accepted February 8, 2015

1 Introduction

Load spectra of aero-engines usually consist of a variety of load parameter matrices. Each of the load parameter matrices corresponds to certain fatigue damage. The load parameter matrices are often obtained by mixing profile load parameter matrices. When the load parameter matrices are obtained by processing the flight profile in an environmental task, they are called environmental mission profile of the load parameter matrices [1]. The collection of various environmental mission profile load parameter matrices is the environmental task load parameter matrices. The environmental task load parameter matrices include cyclic matrix, distribution matrix and correlation matrix. For the cyclic matrix, it includes power cyclic matrix, speed cyclic matrix, torque cyclic matrix, pressure cyclic matrix, overload cyclic matrix, etc. [2]. Cyclic matrix profile parameters represent load cycles, which are used to calculate the low cycle fatigue damage of aero-engines. Measured data used in this paper are the speed cyclic matrix. By extracting peak values, counting parameter cycles and removing invalid cyclic amplitudes of the flight profile, an environmental task parameter cyclic matrix is obtained.

The remainder of this paper is structured as follows. Section 2 reviews several deterministic fatigue life prediction methods that would be used in the following sections and then introduces the procedure of the fatigue life analysis. In Section 3, by analyzing the measured speed cyclic matrix of an aero-engine, the number of the main work cycles of the aero-engine is obtained. In Section 4, based on the cracks in turbine disk mainly caused by low cycle fatigue failures, the loading stress of the turbine disk is analyzed. In Section 5, by fitting the material *S–N* curve, the *S–N* curve of the turbine disk is obtained. In Section 6, by using the *S–N* curve of the turbine disk and Miner's rule, the life of the turbine disk is predicted. In the last section, the conclusions are drawn.

2 Fatigue life prediction methods

According to the irreversibility and randomness of fatigue damages, fatigue life prediction methods can be classified into two groups: deterministic fatigue life prediction methods and probabilistic fatigue life prediction methods [3, 10–12]. In this section, the most commonly used deterministic fatigue life prediction methods are reviewed.

2.1 Stress-based fatigue life prediction methods

Stress-based fatigue life prediction method is one of the earliest developed methods used for fatigue life prediction. The *S–N* curve life prediction is a classic example [4, 9]. Basquin formula is a common fatigue formula used in engineering, which can be expressed as follows [3]:

***Corresponding author: Hong-Zhong Huang,** Institute of Reliability Engineering, University of Electronic Science and Technology of China, No. 2006, Xiyuan Avenue, West Hi-Tech Zone, Chengdu, Sichuan 611731, China, E-mail: hzhuang@uestc.edu.cn
Yan-Feng Li: E-mail: yanfengli@uestc.edu.cn, **Zhiqiang Lv:** E-mail: lvzhiqhappy@126.com, **Wei Cai:** E-mail: 895984547@qq.com, **Shun-Peng Zhu:** E-mail: zspeng2007@uestc.edu.cn, Institute of Reliability Engineering, University of Electronic Science and Technology of China, No. 2006, Xiyuan Avenue, West Hi-Tech Zone, Chengdu, Sichuan 611731, China

$$\sigma_f^{'}(2N_f)^b = \frac{E\Delta\varepsilon_e}{2} = \sigma_a \tag{1}$$

where $\sigma_f^{'}$ is the fatigue strength coefficient, N_f is the fatigue life; b is the fatigue strength exponent, E is the modulus, $\Delta\varepsilon_e$ is the elastic strain range and σ_a is the stress amplitude.

Due to the stress concentration, the stress-based fatigue life prediction method can be further divided into nominal stress method, hot spot stress method and notch stress method.

In this paper, the nominal stress method is used to calculate the low cycle fatigue life of the aero-engines. Material S–N curves are derived from material data and determined by the stress concentration factors. Also, it should be noted that different stress concentration factors correspond to different S–N curves [5].

2.2 Strain-based fatigue life prediction methods

For a heavy service load, during the operation of a component, it is better to use strain–life curve to predict the life of the component. In the 1950s, a second common and more recent approach based on a local strain was established. Manson–Coffin's formula is one of the most commonly used fatigue life prediction methods in engineering. Manson–Coffin's formula describes a relationship between the plastic strain and the fatigue life as follows:

$$\frac{\Delta\varepsilon_p}{2} = \varepsilon_f'(2N_f)^c \tag{2}$$

where $\Delta\varepsilon_p$ is the elastic strain range, ε_f' is the fatigue ductility coefficient, N_f is the fatigue life and c is the fatigue ductility exponent. From eq. (2), it is obvious that $\Delta\varepsilon_p$ determines the value of N_f.

Mason and Hirschberg [6] put forward an improved formula to express the fatigue life by considering the total strain range:

$$\frac{\Delta\varepsilon_t}{2} = \frac{\sigma'_f}{E}(2N_f)^b + \varepsilon_f'(2N_f)^c \tag{3}$$

where $\Delta\varepsilon_t$ is the total strain range, σ_f' is the fatigue strength coefficient, E is the modulus, N_f is the fatigue life, ε_f' is the fatigue ductility coefficient, b is the fatigue strength exponent and c is the fatigue ductility exponent.

2.3 Miner's rule

Suppose that there are L levels of stress in the load spectra [7, 8]. They are denoted as $S_1, S_2, \cdots, S_L$. The number of cycles of each level is denoted as $n_1, n_2, \cdots, n_L$, and the numbers of the destruction cycles of each level are denoted as $N_1, N_2, \cdots, N_L$. Miner's rule assumes that the fatigue damage can be obtained by corresponding circulation ratios. The equation is given as follows:

$$\sum_{i=1}^{L}\frac{n_i}{N_i} = 1 \tag{4}$$

where L is the number of stress levels, n_i is the number of cycles at a given stress level, which can be got from load spectra, N_i is the number of cycles to failure at a given stress level.

A procedure of the fatigue life analysis used in this paper is shown in Figure 1.

First, the S–N curve of the structure should be known. In this paper, the S–N curve of the structure is

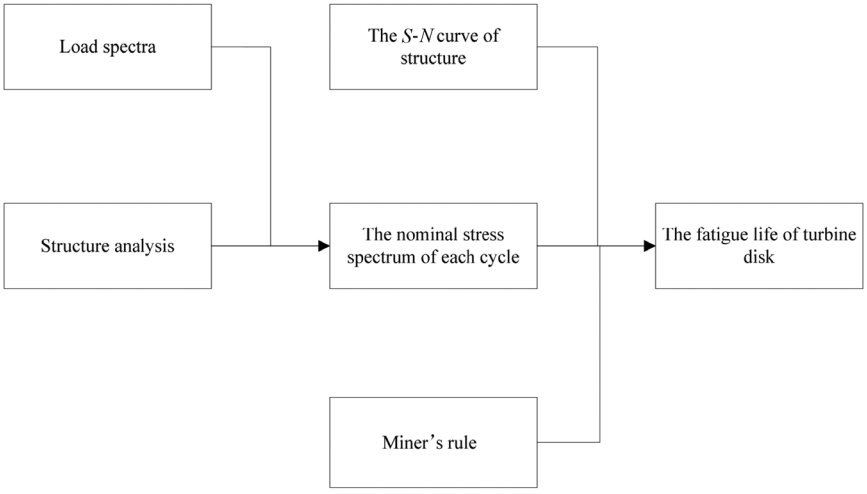

Figure 1: A procedure for the fatigue life analysis of the turbine disk.

obtained by fitting the material data. Second, based on the structure analysis, the nominal stress of each cycle can be represented by S, S_a, S_m and S_{ai}^*. Then the equivalent damage corresponding to each cycle can be calculated. Finally Miner's rule is used to get the fatigue damage and life of the turbine disk.

3 Analysis of speed cyclic matrix data

The measured speed cyclic matrix of an aero-engine of an aircraft is shown in Table 1. The main work cycles can be calculated by analyzing the data in Table 1. Because the data are counted in 2,000 hours many times through the same flight mission, the number of cycles may not be integer. From Table 1, the number of speed cycles of the engines is obtained. Peaks can be defined as four states: take off (>97%), rated take off (94.5–97%), valleys are zero and the ground idle. The numbers of cycles of "0-take off-0," "ground idle-take off-ground idle," "0-rated take off-0" and "ground idle-rated take off-ground idle" are 500.1, 304.8, 221.2 and 420.4. The total number of cycles "0-97%" and "94.5-97%-0" is 721.3, which reflects the flight subjects starting from switch off to take off. The number of cycles of "ground idle-take off state-ground idle" is 725.2, which reflects the flight subjects of landing (but not switching off) to take off again. The number of cycles of "flight idle-take off state-flight idle" is high, which reflects the low frequency using this cycle. Then, the number of the main work cycles of the aero-engine can be obtained and are shown in Table 2.

4 Analysis of turbine disk's loading stress

In this section, the first-stage turbine disk is regarded as objects and their fatigue life is estimated. According to actual turbine disk fracture and related metallographic analysis, the cracks in turbine disk are mainly caused by low cycle fatigue failures.

As shown in Table 1, the centrifugal forces are the main load, which are considered in this paper.

Assuming that the blade's centrifugal forces are evenly distributed on the contact surface of the mortises of the turbine disk, the centrifugal forces are expressed as follows:

$$F = m\omega^2 r \tag{5}$$

where m is the mass of the blades, r is the radius of the center of mass of the blades and ω is the angular velocity of the turbine disk. It means that the loading stress of the turbine disk is proportional to the square of the angular velocity.

Table 1: N_2 cyclic matrix (times, standardization to 2,000 hours).

Peak (%) / Valley (%)	97–100	94.5–97	92.5–94.5	91–92.5	87.5–91	85.5–87.5	81–85.5	75–81	70–75	60–70
0–30	500.1	221.2	62.1	41.7	84.0	30.7	12.5	11.4	13.7	38.0
30–70	304.8	420.4	399.6	322.7	1,713.6	1,680.2	2,034.2	873.8	571.2	93.7
70–75	29.0	34.3	44.2	76.4	346.5	507.0	1,039.1	371.9		
75–81	24.4	122.2	199.6	166.9	1,027.5	1,291.8	2,192.8			
81–85.5	9.0	55.8	88.2	76.9	240.0	79.1				
85.5–87.5	3.1	42.6	87.8	49.0	10.7					
87.5–91	2.7	62.0	66.2							
91–92.5	2.1	3.1								
92.5–94.5	2.1									

Table 2: The number of main work cycles.

Peak		Take off (>97%)		Rated take off (94.5–97%)
Valley	0	Ground idle	0	Ground idle
N_2 cycle number (times)	500.1	304.8	221.2	420.4

5 The fitting of *S–N* curve of the first-stage turbine disk

In this paper, the material *S–N* curve is used to estimate the low cycle fatigue life of the turbine disk for a rough calculation to verify the feasibility of this method. The material used in the test is GH4698 super alloy. The mechanical and fatigue properties of the tested material under the room temperature are listed in Tables 3 and 4, respectively. Considering the influence of stress concentration on turbine disk, the notched fatigue specimen and notched radius are chosen as follows: $\rho = 0.5$ mm, $K_t = 2.33$ for high cycle fatigue; and $\rho_H = 0.25$ mm, $K_t = 3.35$ for low cycle fatigue.

Table 3: Mechanical properties of a GH4698 super alloy.

σ_b(MPa)	$\sigma_{p0.2}$(MPa)	δ%	Ψ%
878	667	15.0	18.0

According to the material's fatigue limit $S_\infty = 1.18 \times 10^8$ Pa, the cycle in the experiment will not cause damage when the stress is less than or equal to 118 MPa. Through the curve fitting, $A = 17.9056$, $\alpha = 0.1945$. Then, the *S–N* curve can be expressed as follows:

$$S = 1.18 \times 10^8 \left(1 + \frac{17.9056}{N^{0.1945}}\right) \tag{6}$$

The *S–N* curve is shown in Figure 2 [13].

6 Fatigue life estimation of the first-stage turbine disk

6.1 Estimation of cyclic stress

The high-pressure rotor speed (N_2) cyclic matrix is shown in Table 1. Assuming that the nominal stress of the first-stage turbine disk is S, it is proportional to the square of the speed N_2:

$$S = k \times N_2^2 \tag{7}$$

where k is the conversion factor. Based on the above assumption, the cyclic stress S is shown in Table 5.

6.2 Estimation of symmetric cyclic stress

After getting the cyclic stress, from the cyclic matrix we can obtain the cyclic stress amplitude S_a as shown in Table 5. After applying the modified Goodman diagram and the *S–N* curve to the experiment data, the stress can be converted into symmetric cyclic stress S_a^*, the modified equation can be expressed as

$$S_a^* = \frac{S_a}{\left(1 - \frac{S_m}{S_b}\right)} = \frac{S_a S_b}{S_b - S_m} \tag{8}$$

where S_a^* is the symmetric cyclic stress, S_a is the amplitude of stress, S_m is the mean stress, S_b is the ultimate strength of the material. To simplify the calculation, we define that $S_b = 878$MPa and the maximum stress of first-stage turbine disk is $S_{\max} = 7.885 \times 10^8$Pa. Then, we can get the corresponding symmetrical cyclic stress, as shown in S_{ai}^* of Table 5.

6.3 Estimation of cumulative damage

The life curve is usually described by the following equation, which is called Goodman diagram:

$$\sigma_a = \sigma_{a0}\left(1 - \frac{\sigma_m}{\sigma_{m0}}\right) \tag{9}$$

where σ_a is the stress amplitude, σ_{a0} is the stress amplitude when the mean is 0, σ_m is the mean stress and σ_{m0} is the mean stress when the amplitude is 0.

The stress cycles of each level can be represented by $(\sigma_{ai}, \sigma_{mi})$ or $(\sigma_{\max i}, R_i)$. Generally, $(\sigma_{\max i}, R_i)$ is accepted in engineering and $\sigma_{\max i}$ can be shorted by σ_i. According to Goodman diagram, (σ_i^*, R_i), which corresponds to (σ_i, R_i) and called symmetrical cyclic stress, can be calculated by the following equation:

Table 4: Fatigue strength of vacuum smelting plus vacuum arc remelting forging.

Heat treatment	θ(°C)	$\sigma_{DH}(R = 0)$(MPa)				σ_{-1H}(MPa)
		10^2 times	5×10^3 times	10^4 times	2×10^7 times	10^8 times
Standard heat treatment	750	981	520	471	118	–

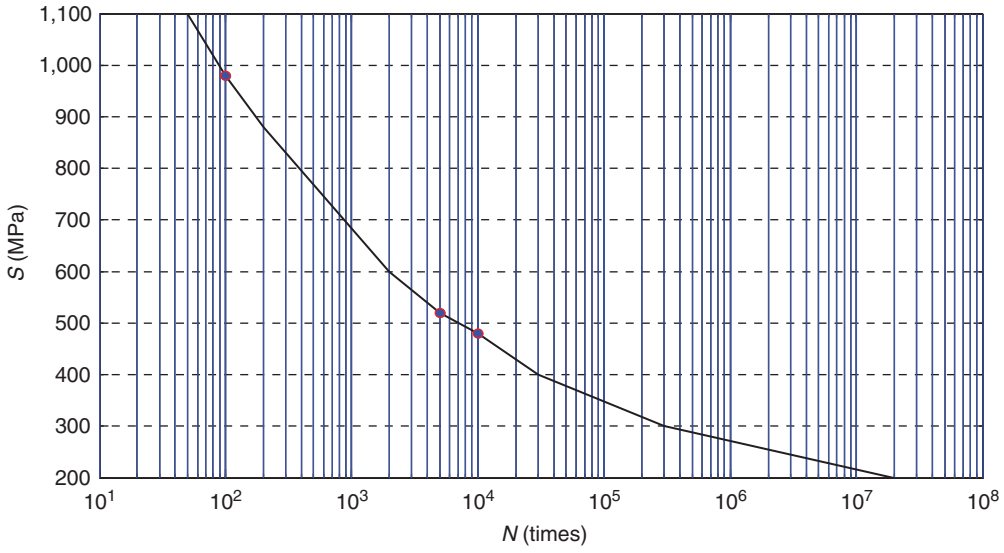

Figure 2: The *S*–*N* curve of a turbine disk.

Table 5: Fatigue limit and damage based on the rotor speeds of aero-engines.

Speed cycle N_2 (%)	Stress cycle S (%)	Stress amplitude S_a (%)	Mean stress S_m (%)	Symmetrical cyclic stress amplitude S_{ai}^* (%)	Fatigue cycle life corresponding N_i	Number of stress cycles n_i	Equivalent damage corresponding D_i
0–98.5	0–97.0225	48.51125	48.51125	69.85929	40,455	500.1	0.013178
60–98.5	36–97.0225	30.51125	66.51125	52.51266	393,220	304.8	0.000691
72.5–98.5	52.5625–97.0225	22.23	74.7925	42.03376	3,230,106	29.0	5.88E-06
78–98.75	60.84–97.0225	18.09125	78.93125	35.98176	19,116,698	24.4	1.80E-06
83.25–98.75	69.30563–97.0225	13.85844	83.16406	29.10668	$>2\times10^7$	9.0	0
86.5–98.75	74.8225–97.0225	11.1	85.9225	24.19621	$>2\times10^7$	3.1	0
89.25–98.75	79.65563–97.0225	8.683438	88.33906	19.57815	$>2\times10^7$	2.7	0
91.75–98.75	84.18063–97.0225	6.420937	90.60156	14.95764	$>2\times10^7$	2.1	0
93.5–98.75	87.4225–97.0225	4.8	92.2225	11.4541	$>2\times10^7$	2.1	0
0–95.75	0–91.68063	45.84031	45.84031	64.45137	74,266	221.2	0.003248
60–95.75	36–91.68063	27.84031	63.84031	46.56727	1,166,887	420.4	0.000343
72.5–95.75	52.5625–91.68063	19.55906	72.12156	35.8431	20,074,850	34.3	1.21E-06
78–95.75	60.84–91.68063	15.42031	76.26031	29.67645	$>2\times10^7$	122.2	0
83.25–95.75	69.30563–91.68063	11.1875	80.49313	22.69497	$>2\times10^7$	55.8	0
86.5–95.75	74.8225–91.68063	8.429063	83.25156	17.72396	$>2\times10^7$	42.6	0
89.25–95.75	79.65563–91.68063	6.0125	85.66813	13.06066	$>2\times10^7$	62.0	0
91.75–95.75	84.18063–91.68063	3.75	87.93063	8.406192	$>2\times10^7$	3.1	0
0–93.5	0–87.4225	43.71125	43.71125	60.32048	124,639	62.1	0.000458
60–93.5	36–87.4225	25.71125	61.71125	42.06249	3,207,156	399.6	0.000126
72.5–93.5	52.5625–87.4225	17.43	69.9925	31.17526	$>2\times10^7$	44.2	0
78–93.5	60.84–87.4225	13.29125	74.13125	24.93546	$>2\times10^7$	199.6	0
83.25–93.5	69.30563–87.4225	9.058438	78.36406	17.88924	$>2\times10^7$	88.2	0
86.5–93.5	74.8225–87.4225	6.3	81.1225	12.8838	$>2\times10^7$	87.8	0
89.25–93.5	79.65563–87.4225	3.883438	83.53906	8.196997	$>2\times10^7$	66.2	0
0–91.75	0–84.18063	42.09031	42.09031	57.27656	189,305	41.7	0.000115
60–91.75	36–84.18063	24.09031	60.09031	38.76319	7,820,072	322.7	4.38E-05
72.5–91.75	52.5625–84.18063	15.80906	68.37156	27.76891	$>2\times10^7$	76.4	0

(*continued*)

Table 5: (*Continued*)

Speed cycle N_2 (%)	Stress cycle S (%)	Stress amplitude S_a (%)	Mean stress S_m (%)	Symmetrical cyclic stress amplitude S_{ai}^* (%)	Fatigue cycle life corresponding N_i	Number of stress cycles n_i	Equivalent damage corresponding D_i
78–91.75	60.84–84.18063	11.67031	72.51031	21.48292	$>2\times10^7$	166.9	0
83.25–91.75	69.30563–84.18063	7.4375	76.74313	14.39777	$>2\times10^7$	76.9	0
86.5–91.75	74.8225–84.18063	4.679063	79.50156	9.373181	$>2\times10^7$	49.0	0
0–89.25	0–79.65563	39.82781	39.82781	53.16662	353,418	84.0	0.000181
60–89.25	36–79.65563	21.82781	57.82781	34.33525	35,291,322	1713.6	4.91E-05
72.5–89.25	52.5625–79.65563	13.54656	66.10906	23.21366	$>2\times10^7$	346.5	0
78–89.25	60.84–79.65563	9.407813	70.24781	16.87534	$>2\times10^7$	1027.5	0
83.25–89.25	69.30563–79.65563	5.175	74.48063	9.748973	$>2\times10^7$	240.0	0
86.5–89.25	74.8225–79.65563	2.416563	77.23906	4.706529	$>2\times10^7$	10.7	0
0–86.5	0–74.8225	37.41125	37.41125	48.94609	734,302	30.7	1.73E-05
60–86.5	36–74.8225	19.41125	55.41125	29.81994	$>2\times10^7$	1680.2	0
72.5–86.5	52.5625–74.8225	11.13	63.6925	18.58771	$>2\times10^7$	507.0	0
78–86.5	60.84–74.8225	6.99125	67.83125	12.20728	$>2\times10^7$	1291.8	0
83.25–86.5	69.30563–74.8225	2.758438	72.06406	5.051641	$>2\times10^7$	79.1	0
0–83.25	0–69.30563	34.65281	34.65281	44.32939	1,881,000	12.5	5.05E-06
60–83.25	36–69.30563	16.65281	52.65281	24.91724	$>2\times10^7$	2034.2	0
72.5–83.25	52.5625–69.30563	8.371563	60.93406	13.5867	$>2\times10^7$	1039.1	0
78–83.25	60.84–69.30563	4.232813	65.07281	7.173193	$>2\times10^7$	2192.8	0
0–78	0–60.84	30.42	30.42	37.63102	11,045,325	11.4	6.70E-07
60–78	36–60.84	12.42	48.42	17.8708	$>2\times10^7$	873.8	0
72.5–78	52.5625–60.84	4.13875	56.70125	6.438402	$>2\times10^7$	371.9	0
0–72.5	0–52.5625	26.28125	26.28125	31.49541	$>2\times10^7$	13.7	0
60–72.5	36–52.5625	8.28125	44.28125	11.48483	$>2\times10^7$	571.2	0
0–65	0–42.25	21.125	21.125	24.36766	$>2\times10^7$	38.0	0
60–65	36–42.25	3.125	39.125	4.14709	$>2\times10^7$	93.7	0

$$\sigma_i^* = \frac{(1-R_i)\sigma_{m0}\sigma_i}{\sigma_{m0}(1-R_i^*)+S_i(R^*-R_i)} \tag{10}$$

Then S–N curve and eq. (10) are used to calculate the fatigue life which corresponds to (σ_i, R_i), the fatigue life is

$$N_i = \left(\frac{S_\infty A}{\sigma_i^* - S_\infty}\right)^{\frac{1}{\alpha}} \tag{11}$$

If S_i is known, the corresponding fatigue life can be calculated by

$$N_i = \left(\frac{AS_\infty}{S_i - S_\infty}\right)^{\frac{1}{\alpha}} \tag{12}$$

Substituting parameters into eq. (12) with $S_\infty = 1.18\times 10^8$Pa, $A = 17.9056$, $\alpha = 0.1945$

$$N_i = \left(\frac{2.1128608\times10^9}{S_i - 1.18\times10^8}\right)^{5.141388} \tag{13}$$

The corresponding cyclic life by eq. (13) is shown in Table 5.

Then by using the Miner's rule, we substitute parameters into eq. (12) $S_\infty = 1.18\times10^8$Pa, $A = 17.9056$, $\alpha = 0.1945$, and instead of S_i by S_a^*, the D_{total} is

$$\begin{aligned} D_{\text{total}} &= \sum_{i=1}^{k}\frac{n_i}{N_i} \\ &= \sum_{i=1}^{k}\frac{n_i}{\left[\dfrac{2.1128608\times10^9}{S_{ai}^* - 1.18\times10^8}\right]^{5.141388}} \end{aligned} \tag{14}$$

Cyclic life N_i and equivalent damage D_i are shown in Table 5, and $D_{\text{total}} = 0.018471$.

According to the calculation, the cumulative fatigue damage is 0.018471 after 2,000 flight hours. It indicates that although the main failure mechanisms of the turbine disc are low cycle fatigue, the total damage of the turbine disk is small which is caused by the centrifugal forces in 2,000 flight hours. It should be noted that, in the operation of the turbine disk, it also endures high thermal stresses. But because of the

lack of experimental data, in this paper, only the centrifugal forces are used to estimate the life of the turbine disk. So we will do further study about the life of the turbine disk in the future.

7 Conclusions

In this paper, based on the actual measured load spectra speed cyclic matrix, the fatigue life of the first-stage turbine disk was estimated. The experimental results demonstrated that the centrifugal forces are the main load of the turbine disk. Also, it is clear that the *S–N* curve and Miner's rule can be used to estimate the fatigue life of the turbine disk. Similarly, this method can be used to estimate the fatigue life of the other components of the aero-engine. But it should be noted that, when just considering the centrifugal forces of the loading stress, the total damage of the turbine disk is small. In order to have a high precision of fatigue life estimation of the turbine disk, more experimental data about the loading stress are need. Also, the life estimation method can be further improved if there are more accurate parameters.

Funding: The authors would like to acknowledge the partial support provided by the National Natural Science Foundation of China under contract number 11272082 and the Fundamental Research Funds for the Central Universities under contract number E022050205.

References

1. Su QY. Guide of determining life of aviation turbojet, turbofan engine main parts. Beijing: Aviation Industry Press, 2004.
2. Raiher VL. Some consequences from the two parameters model of durability scatter. Uchenve Zapiski CAHI 1982;13:130–3.
3. Zhu SP. Research on hybrid probabilistic physics of failure modeling and fatigue life estimation of high-temperature structures. Ph.D. Dissertation, University of Electronic Science and Technology of China, 2011.
4. Cui W. A state-of-the-art review on fatigue life prediction methods for metal structures. J Mar Sci Technol 2002;7:43–56.
5. Yao WX. The fatigue life analysis of structure. Beijing: National Defense Industry Press, 2003.
6. Mason SS, Hirschberg MH. Fatigue: an interdisciplinary approach. Syracuse, NY: Syracuse University Press, 1964.
7. Miner MA. Cumulative damage in fatigue. J Appl Mech 1945;12:159–64.
8. Hashin Z, Rotem A. A cumulative damage theory of fatigue failure. Mater Sci Eng 1978;34:147–60.
9. Wirsching PH. Fatigue reliability for offshore structures. J Struct Eng 1984;100:2340–56.
10. Zhu SP, Huang HZ, Wang ZL. Fatigue life estimation considering damaging and strengthening of low amplitude loads under different load sequences using fuzzy sets approach. Int J Damage Mech 2011;20:876–99.
11. Zhu SP, Huang HZ, Ontiveros V, He LP, Modarres M. Probabilistic low cycle fatigue life prediction using an energy-based damage parameter and accounting for model uncertainty. Int J Damage Mech 2012;21:1128–53.
12. Zhu SP, Huang HZ, He LP, Liu Y, Wang Z. A generalized energy-based fatigue-creep damage parameter for life prediction of turbine disk alloys. Eng Fract Mech 2012;90:89–100.
13. Fu N. An aircraft engine turbine disk and blade strength analysis and calculation of life. M.D. Dissertation, Northwestern polytechnic University, 2006.